

THE OUTER HELIOSPHERE: SOLAR WIND, COSMIC RAY AND VLF RADIO EMISSION VARIATIONS

Ralph L. McNutt, Jr.

The Johns Hopkins University Applied Physics Laboratory Laurel, MD 20723 USA

Launched in August and September of 1977, the Voyager 1 and 2 spacecraft are now > 45 astronomical units (AU) from Earth. Both spacecraft continue to monitor the outer heliosphere fields-and-particles environment on a daily basis during their journey to the termination shock of the solar wind. Strong transient shocks continue to be detected in the solar wind plasma. The largest of these are associated with Global Merged Interaction Regions (GMIRs) which, in turn, block cosmic ray entry into the inner heliosphere and are apparently responsible for triggering the two major episodes of VLF radio emissions now thought to come from the heliopause. Distance estimates to the termination shock are consistent with those determined from observations of anomalous cosmic rays. Current observations and implications for heliospheric structure are discussed.

Knowledge of the Outer Heliosphere

The heliosphere is the plasma cavity blown out by the solar wind in the Very Local Interstellar Medium (VLISM)^{1,2}. The outer heliosphere can be defined roughly as that part of the cavity extending from the orbit of Neptune (roughly 30 AU from the Sun) through the interaction region with the VLISM. This region has been directly accessible to solar-system-escaping spacecraft - Pioneer 10 and 11 and Voyager 1 and 2 - for less than the last decade. During this time direct measurements of the local medium have been possible. Typical values and variabilities of the solar wind plasma, interplanetary magnetic field and relevant derived quantities are shown in Table 1.

Table 1. Solar Wind at 30-50 AU

Parameter		Typical Value	Variability ^a
Magnetic Field	B	0.2 nT	x2
Solar Wind Speed	V_{sw}	450 km s ⁻¹	± 75 km s ⁻¹
Proton Density	n_{proton}	@ 30 AU 0.01 cm ⁻³ @ 50 AU 0.004 cm ⁻³	x2
Ram Pressure	ρV_{sw}^2	2×10^{-11} dyne cm ⁻²	x2
Proton Temperature	T_i	1.3 eV 15,000 K	± 0.4 eV ± 5000 K
Mach #	$M \equiv V_{sw} / (2kT_i/m_p)^{1/2}$	~45	x2
Alfvén Mach #	$M_A \equiv V_{sw} / (B^2/4\pi n_p m_p)^{1/2}$	~10	x2
Sonic Mach #	$M_s \equiv V_{sw} / (kT_e/m_p)^{1/2}$	~30	x2
CH ₄ + gyro radius	r_{pu} (CH ₄ +)	30,000 km $\approx 300 R_{pluto}$	
Proton gyro radius	r_{gyro} (proton)	600 km	
Electron gyro radius	r_{gyro} (electron)	10 km	
Bow Shock Width ^b	$r' = V_{sw} / \Omega_{ci}$	23,000 km $\approx 20 R_{gyro}$	

^a Changes that can be expected on a time scale of days. (x2 means a factor of two).

^b The effective gyro radius of upstream protons whose bulk motion (V_{sw}) is converted to gyro motion at the shock (Bagenal, F., J. W. Belcher, E. C. Sittler and R. P. Lepping, The Uranian bow shock; Voyager 2 inbound observations of a high Mach number shock, *J. Geophys. Res.*, 92, 8603, 1987.)

This current fleet of spacecraft are spread out in both heliographic latitude and longitude, and have allowed us our first look at the symmetries and asymmetries present in the particles and fields properties of the global heliospheric system (Table 2). As shown in Figure 1, Voyager 1 and 2 and Pioneer 11 (no longer actively tracked) cover heliospheric longitudes centered around the incoming direction of the neutral component of the interstellar wind³). Similarly, latitudinal coverage includes Pioneer 10 near the heliographic equatorial plane and Voyager 1 and Voyager 2 at northern and southern heliographic latitudes, respectively.

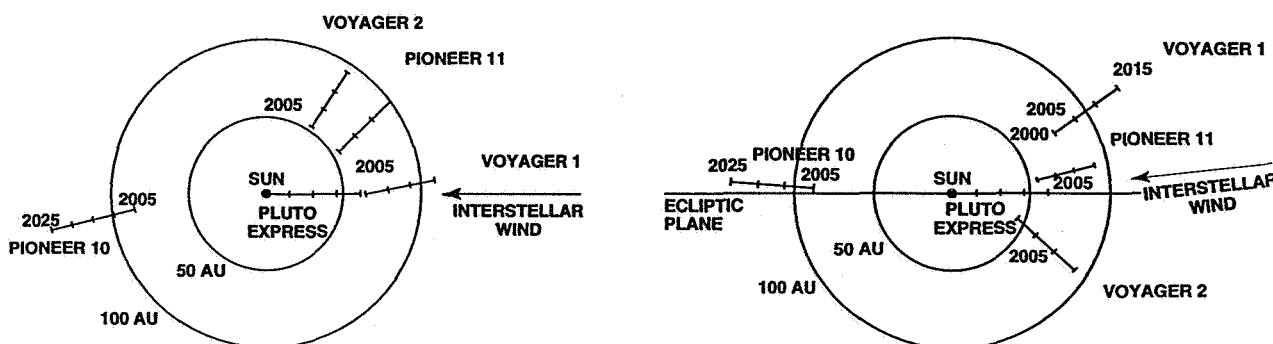


Figure 1. Cruise Trajectories. *Left*: Ecliptic plane projection of spacecraft trajectories and interstellar wind velocity vector. *Right*: Latitudinal scan of the same trajectories.

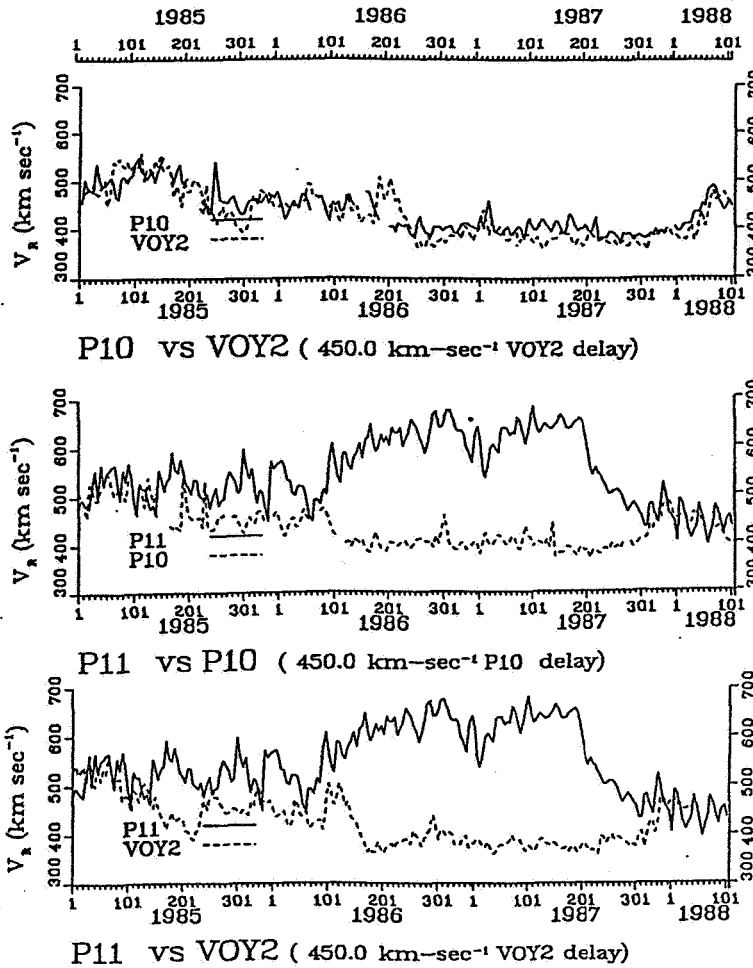
Table 2. Outer Heliosphere Spacecraft

Spacecraft	Launch	Cruise Science	Mission
Pioneer 10	3 March 1972 Atlas Centaur	Yes	Jupiter Flyby: 12/4/73 Prop. Term.: FY99
Pioneer 11	5 April 1973 Atlas Centaur	Yes	Jupiter Flyby: 12/3/74 Saturn Flyby: 9/1/79 Prop Term.: FY96
Voyager 1	5 Sept. 1977 Titan III D Centaur	Yes	Jupiter: 3/5/79, Saturn: 7/9/80 ~ 150 AU in 2020
Voyager 2	20 Aug. 1977 Titan III D Centaur	Yes	Jupiter: 7/9/79, Saturn: 8/26/81, Uranus: 1/24/86, Neptune: 8/25/89 ~ 130 AU in 2020
Galileo	18 Oct. 1989 STS/IUS	No	Jupiter Orbit: 12/7/95 – 11/7/97
Cassini (In Development)	6 Oct. 1997 Titan IV Centaur	Not Planned	Saturn Orbit: 6/25/04 – 6/25/08
Pluto Express (Proposed)	2003 Proton Direct; Delta/Molniya JGA	Not Planned	~ 2013+ Pluto Flyby and Kuiper Belt Object E Encounter
Small Interstellar Probe (Proposed)	~2010 Various	Yes Primary	To ~200 AU (~ 2025 AE 2035)

The table lists all spacecraft flown and planned to fly past the asteroid belt. Few interplanetary measurements were made by Galileo enroute to Jupiter and none are planned for Cassini enroute to Saturn. Pluto Express is a smaller version of Pluto Fast Flyby and the Small Interstellar Probe is a study concept.

This coverage reveals that in the outer heliosphere, the solar wind appears cylindrically symmetric. Multi-year observations of the solar wind radial velocity component (Figure 3) show essentially the same long-term structure at both Voyager 2 and Pioneer 10 when the two spacecraft were at similar latitudes but separated by 180° in longitude. At the same time comparison of Pioneer 10 vs Pioneer 11 and Pioneer 10 vs Voyager 2 show a difference of ~ 200 km/s during the time around the solar minimum during the last decade. It is now clear from Ulysses observations that the higher speed wind as observed at the higher latitude Pioneer 11 spacecraft is that associated with the northern hemisphere coronal hole⁴). During solar minimum the hole structure becomes more ordered and the difference in latitude more pronounced⁵).

Transients in the solar wind also continue to be observed far from the Sun. The most pronounced event was seen by the PLS experiment on Voyager 2 around day 146



Same Latitude
180° Different Longitudes

Different Latitude
180° Different Longitudes

Different Latitude
Same Longitudes

Figure 3. Solar Wind Latitude Effects. Solar wind variations in latitude and longitude show that the primary solar wind structure is latitudinal.

of 1991 when the spacecraft was located at 35 AU. A strong shock was observed propagating outward at 550 km/s⁶). Following the shock passage by about 14 days was a period of “double streaming,” i.e., there were literally two different interpenetrating streams of solar wind. This is a condition observed closer to Earth when there is a radial turning of the interplanetary magnetic field⁷). In the case here, the shock and transient appear to have blown the field lines into a radial configuration, allowing the interpenetration of the solar wind streams, which are collisionless and can only typically interact via the mediation of the ambient magnetic field.

Energetic Particles

The shocks associated with such transients as well as with corotating interaction regions and the more encompassing global merged interaction regions (GMIRs)⁸) accelerate ions and electrons in the medium to suprathermal (10s of keV and up) energies.

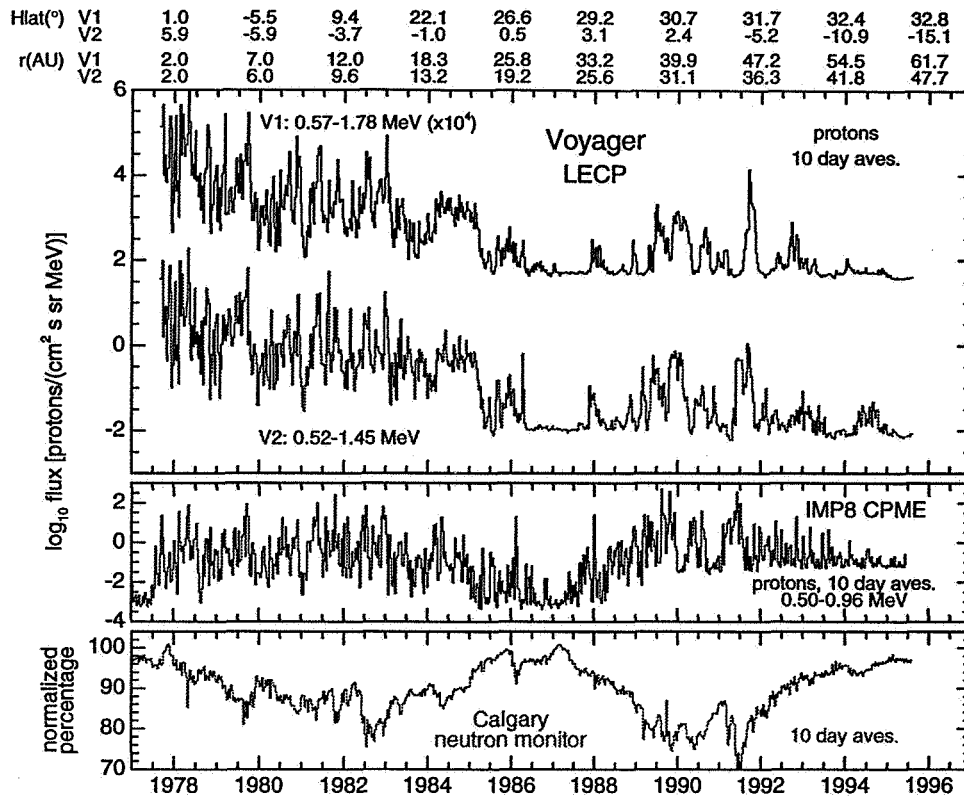


Figure 4. Energetic particle population in the heliosphere from 1977 through 1995.

An overview of the energetic particle observations measured by the Voyager LECP experiments is shown in Figure 4⁹⁾. The top two traces show the differential flux of ~0.5 to 1.5 MeV protons at the two Voyager spacecraft. The center trace shows intensities in a similar energy range measured with similar instrumentation on the IMP 8 spacecraft. The latter is in Earth orbit (in a roughly circular orbit at 30 Earth radii) and provides a 1 AU baseline for analyzing the measurements in the outer heliosphere. The bottom trace shows the variation of neutrons at the ground. The solar cycle is clearly seen in both the neutron monitor and IMP 8 data.

A closer look at the variations in the energetic particle population shows a clear correlation with changes in solar wind speed (shocks produced by CIRs or transients - see Figure 5)¹⁰⁾.

Comparison of solar wind speed, cosmic ray flux, and energetic particle populations show that these observables are connected globally in the heliosphere. The bottom panel of Figure 6 shows the solar wind speed profile at Voyager 2. The strong transient shock referred to previously is the most striking feature present⁹⁾. The second panel from the bottom shows energetic particles in three different energy ranges measured at the same spacecraft. There is a prominent enhancement at the time of the solar wind shock; however, a stronger enhancement is seen ~4 months later (labeled as Sept. '91). This

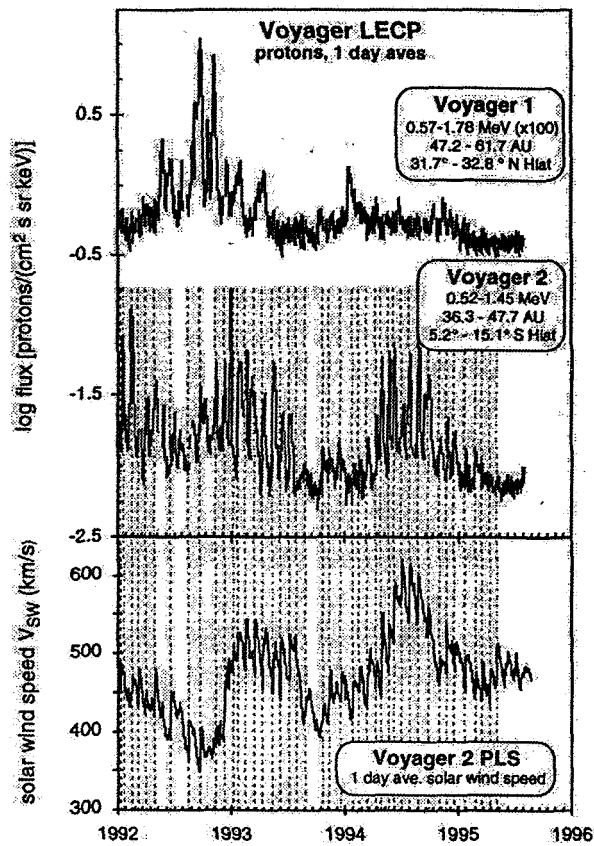


Figure 5. Local energetic particle intensities and solar wind speed. The top two traces show the observed energetic particle fluxes at Voyager 1 and Voyager 2. Differences are ascribed primarily to the difference in heliolatitude of the two spacecraft. The dashed lines connecting the bottom two traces show a notable correspondence between the location of energetic particles and jumps observed in the solar wind speed. A similar comparison at Voyager 1 is not possible due to an instrument malfunction with the Voyager 1 PLS experiment following the Saturn flyby in November 1980.

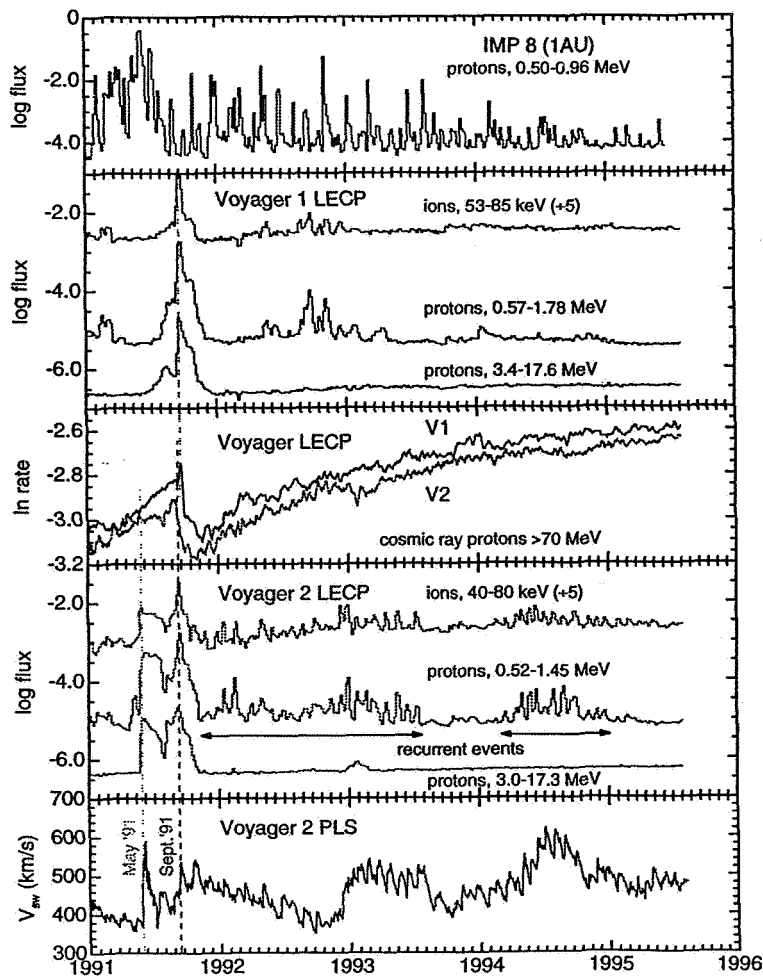


Figure 6. Energetic particle intensities in the indicated energy range from IMP 8, Voyager 1 and Voyager 2, together with cosmic ray intensities ($E_{\text{proton}} > 70$ MeV) at Voyager 1 and Voyager 2. The solar wind plasma speed at Voyager 2 is also shown as are the May and September 1991 shocks seen at the Voyager 2 spacecraft.

enhancement is also associated with a solar wind shock, but not such a prominent one. However, as the dashed line shows, the September 1991 shock also produced energetic particle enhancements at Voyager 1 located > 10 AU away. Also, this event produced a Forbush decrease, a major drop in the flux of cosmic rays at both the Voyager 1 and 2 spacecraft. Such decreases are typically produced by magnetic barriers - regions of compressed and tangled magnetic fields associated with GMIRs. The global nature of the September 1991 shock and its identification as a GMIR is evidenced by heightened energetic particle populations at the two Voyager spacecraft as well as the (global) heliospheric drop in cosmic ray intensity¹¹⁾. This is in sharp contrast to the shock seen at Voyager 2 in late May which is now easily seen to be a very spatially-confined transient event. The shock in May can be traced back to solar activity in March 1991 while the September shock can be traced back to activity in June 1991. The latter activity was more intense and/or widespread at the Sun, resulting in a major heliospheric disturbance. This activity appears also to have associated with it an anomalously high neutrino counting rate in the Homestake experiment which has led to renewed speculation regarding a connection between observed solar neutrinos and solar activity^{12,13)}.

Heliospheric Radio Emission

In 1983 Very Low Frequency (propagating) radio emissions were detected at both Voyager 1 and 2 by the Plasma Wave Systems (PWS) experiment¹⁴⁾. The origin and transient nature of the emissions were a mystery; it was suggested that the emissions were somehow 'triggered' by anomalously strong solar activity^{15,16)}. This trigger hypothesis has been confirmed by another episode of intense emissions between 2 and 3 kHz and measured during 92-93^{6,17)}. The emissions have been interpreted as coming from the direction of the incoming interstellar wind where the plasma density is increased over ambient values by the obstacle presented to the flow by the outflowing solar wind¹⁷⁾.

Timing of the emissions versus knowledge of the disturbance responsible for them can be used to estimate the distance to the emitting region^{15,16)}. The responsible shock passed Voyager 2 on day 251 of 1991 at a speed of 548 km/s. Allowing for the slowing of the shock as it piles up material in front of it leads to a distance of ~ 110 to 130 AU to the emission area¹⁶⁾.

Since 1980 only two episodes of solar activity have been sufficiently strong to produce strong VLF emissions. Only the second episode appears to be associated with a possibly anomalous solar neutrino flux^{12,13)}.

Prior to 1980 these emissions could not be detected as no spacecraft were in regions of the solar wind where the *in situ* plasma (lower cutoff) frequency was less than the VLF emission frequency. The emissions are only observable at heliocentric distances of ~ 10 AU (about the orbital distance of Saturn and beyond).

Anomalous Cosmic Rays

The anomalous component of cosmic rays consists of an upturning in the cosmic ray spectrum at energies of tens of MeV per nucleon (Figure 7)¹⁸⁾. This cosmic ray component has been detected in elements thought to be present as neutral atoms in the VLISM. Measurements of the charge state show this component to be singly ionized as compared with the highly stripped galactic component. Both the increasing intensity and the charge state confirm the idea that the anomalous component is a heliospheric phenomenon locally produced by photoionization of neutral interstellar gas atoms by the Sun¹⁹⁾. The ionized material is subsequently picked up by the solar wind²⁰⁾ convective electric field and transported to the termination shock. At the shock, the particles are accelerated by the shock-associated electric field before diffusing back into the heliospheric cavity where they are detected by the spacecraft (Figure 8). The increase of energy density with heliospheric distance has led to speculation that the termination shock is modified in a self-consistent manner by the acceleration process²¹⁾.

The anomalous component is thus an extra radiation source produced by the interaction of the heliosphere with the VLISM. Such a radiation source may play a role

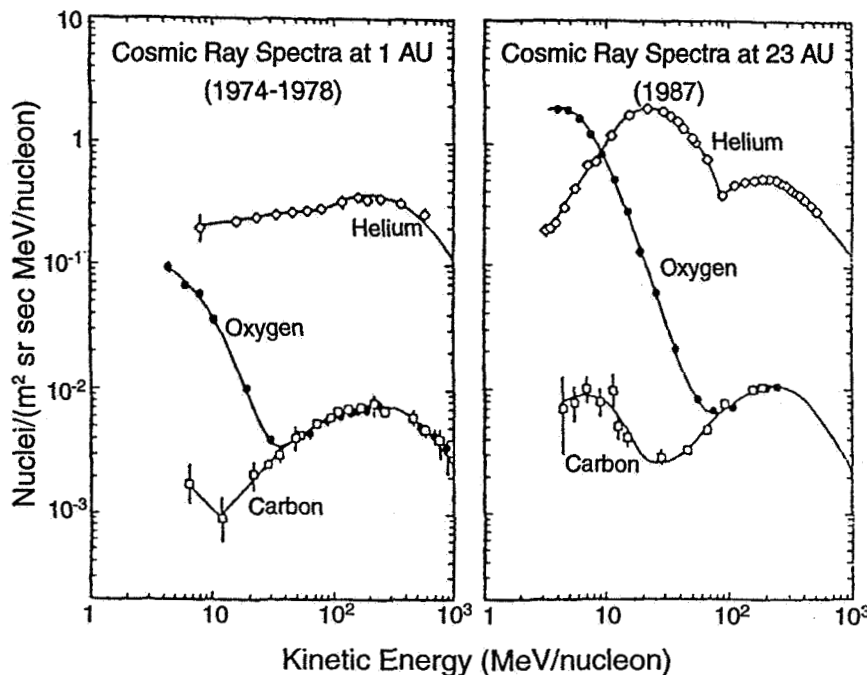


Figure 7. The energy spectra of helium, oxygen, and carbon measured near 1 AU and 23 AU. The increase at lower energies in the outer solar system is due to anomalous cosmic rays.

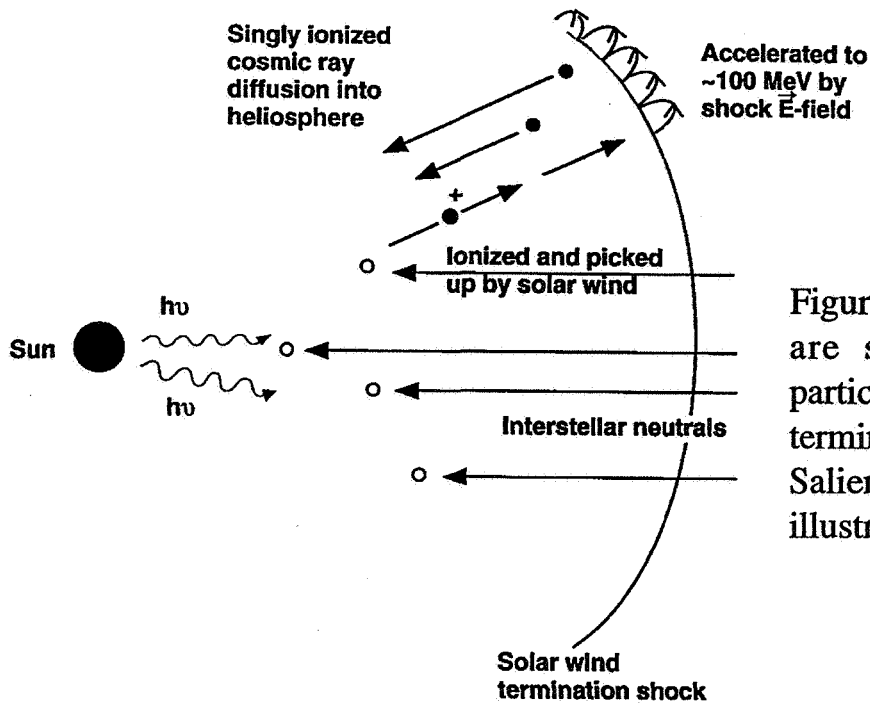


Figure 8. Anomalous cosmic rays are singly-charged energetic particles that are accelerated at the termination shock of the solar wind. Salient features of this process are illustrated in the sketch.

in surface material processing of outer heliosphere objects. Radiation darkening²²⁾ could account for the reddening of spectra of outer heliosphere objects such as 5145 Pholus and perhaps Pluto²³⁾ and other Kuiper belt objects²⁴⁾. The extent of processing of these materials by the heliospheric environment may yield important clues to the evolution of the solar nebula. One could even speculate as to whether the anomalous component could have played a role in the processing of organic to prebiotic material at some past epoch.

Summary and Conclusions

The continuing missions of Voyager and Pioneer show that the outer heliosphere (>50 AU) is dynamic and exhibits behavior driven by changing input conditions at the Sun. The far solar wind retains structure and exhibits both compression and rarefaction regions. Unambiguous signatures of deceleration and heating that are expected near the termination shock have not been found. There has been no direct detection of the termination shock by either Voyager 1 or 2 (at heliospheric distances of 61.012 AU = 8.4570 light hours and 47.126 AU = 6.5323 light hours, 23 October 1995, respectively).

The incoming neutral component of VLISM is known from Lyman- α measurements. Pick-up interstellar ions are directly observed by the Ulysses spacecraft. Local particle acceleration is still seen at CIRs and in transients (GMIRs), and the energy density in anomalous cosmic rays continues to increase. The triggering of VLF emissions from the heliopause region is now established and linked back to solar activity.

We have come a long way since the initial speculation about the interaction of the solar wind with interstellar space^{1,25}). The heliosphere remains full of new discoveries as the robotic arms of the human race continue their outward reach.

Acknowledgments

This work was supported under NASA Grant NAGW-4603 as part of the Voyager Interstellar Mission via Task I of Contract N00039-95-C-002 and via MIT under subcontract purchase order SV-C-600220. The author acknowledges the contributions and support of the JHU/APL Publications and Reports Group, especially Barbara Northrop, Carole Gaither and Elin Frye.

References

- 1) E. N. Parker, *Interplanetary Dynamical Processes* (John Wiley, NY, NY, 1963).
- 2) P. C. Frisch, *Science* **265**, 1423 (1994).
- 3) R. Lallement, J-L. Bertaux, and J. T. Clarke, *Science* **260**, 1095 (1993).
- 4) Phillips *et al.*, *Geophys. Res. Lett.* **22**, 3301 (1995).
- 5) P. R. Gazis, *Geophys. Res. Lett.* **21**, 1743 (1994).
- 6) R. L. McNutt, Jr. *et al.*, *Adv. Space Res.* **16**(9), 303 (1995).
- 7) W. C. Feldman *et al.*, *Rev. Geophys. Space Phys.* **12**, 715 (1974).
- 8) L. F. Burlaga *et al.*, *J. Geophys. Res.* **90**, 12027 (1985).
- 9) S. M. Krimigis *et al.*, *Proc. 24th International Cosmic Ray Conf.*, **4**, 401 (1995).
- 10) R. B. Decker *et al.*, *Proc. 24th International Cosmic Ray Conf.*, **4**, 421 (1995).
- 11) F. B. McDonald *et al.*, *J. Geophys. Res.* **99**, 14705 (1994).
- 12) R. Davis, *Prog. Part. Nucl. Phys.* **32**, 13 (1994).
- 13) R. L. McNutt, Jr., *Science* **270**, 1635 (1995).
- 14) W. S. Kurth *et al.*, *Nature* **312**, 27 (1984).
- 15) R. L. McNutt, Jr., *Geophys. Res. Lett.* **15**, 1307 (1988).
- 16) R. L. McNutt, Jr., *Adv. Space Res.* **9**(4), 235 (1989).
- 17) D. A. Gurnett *et al.*, *Science* **262**, 199 (1993).
- 18) T. Holzer *et al.*, *The Interstellar Probe: Scientific Objectives and Requirements for a Frontier Mission to the Heliospheric Boundary and Interstellar Space* (California Institute of Technology, Pasadena, CA, 1990).
- 19) L. A. Fisk, B. Kozlovsky, and R. Ramaty, *Astrophys. J.* **190**, L35 (1974).
- 20) G. Gloeckler *et al.*, *J. Geophys. Res.* **99**, 17637 (1994).
- 21) G. P. Zank *et al.*, *J. Geophys. Res.* **99**, 14729 (1994).
- 22) W. R. Thompson *et al.*, *J. Geophys. Res.* **92**, 14933 (1987).
- 23) F. Bagenal *et al.*, *Pluto/Charon* (Univ. of Arizona Press, Tucson, AZ, in press, 1996).
- 24) A. L. Cochran *et al.*, *Astrophys. J.* **455**, 342 (1995).
- 25) L. Davis, Jr., *Phys. Rev.* **100**, 1440 (1955).